Tetrahedron 67 (2011) 4243–4252

Contents lists available at ScienceDirect

Tetrahedron

journal homepage: www.elsevier.com/locate/tet

Suzuki–Miyaura cross-coupling reaction on copper-*trans*-A_2B corroles with excellent functional group tolerance

Michael König [a], Lorenz Michael Reith [a], Uwe Monkowius [a], Günther Knör [a], Klaus Bretterbauer [b], Wolfgang Schoefberger [a,*]

[a] Institute of Inorganic Chemistry, Johannes Kepler University Linz (JKU), Altenberger Straße 69, A-4040 Linz, Austria
[b] Institute of Chemical Technology of Organic Substances, Johannes Kepler University Linz (JKU) Altenberger Straße 69, A-4040 Linz, Austria

ARTICLE INFO

Article history:
Received 7 March 2011
Received in revised form 29 March 2011
Accepted 7 April 2011
Available online 14 April 2011

Keywords:
Corrole
Copper
Suzuki–Miyaura coupling reaction
Pd-catalysts
Boronic acids/esters
Density functional theory (DFT)
Time-dependent DFT

ABSTRACT

The palladium-catalyzed Suzuki–Miyaura cross-coupling reaction has been investigated on *meso*-substituted *trans*-A_2B-corrole using tailored Pd-catalyst systems.
We present the first examples of Suzuki–Miyaura cross-coupling reactions on *meso*-substituted *trans*-A_2B-corrole derivatives with neutral, sterically hindered, inactivated and heteroaromatic boronic acids and esters, alkenylboronic acids, as well as quickly deboronating aryl boronic acids and benzo-condensated five membered heterocyclic boronic acids. In addition, we established a high-yield procedure for the Suzuki–Miyaura cross-coupling reaction of corroles with neutral boronic acids.
Due to the lability of the free-base corrole macrocycles, functionalization of the corrole periphery was performed with the corresponding Cu-metallated species. *meso*-Substituted *trans*-A_2B-corrole can hence be regarded as highly versatile platform towards more sophisticated corrole systems.
X-ray structure analysis of a functionalized *meso*-substituted *trans*-A_2B copper corrole exhibited the typical features of such a Cu-complex: short N–Cu distances and a saddled corrole configuration.
Moreover, we observed a sensitivity of the formal oxidation state of the coordinated copper ions towards Suzuki–Miyaura cross-coupling reaction conditions, where the central copper(III) ion approaches the characteristic features of a copper(II) species. This redox behaviour was examined by UV/vis absorption spectra, nuclear magnetic resonance (NMR) experiments and time-dependent density functional theoretical calculations.

1. Introduction

The demand of synthesizing novel symmetric and asymmetric corroles increased significantly over the past decade. This trend was triggered by the first published one-pot synthesis of corroles reported in 1999 by Gross and Paolesse.[1–4] Since then, the scope of corrole application grew tremendously including examples in the fields of catalysis, photochemical sensors, molecular electronics and biomedicinal applications.[5] For these purposes the availability of more sophisticated corrole systems is of great interest, which resulted in various contributions on corrole functionalization, including reactions on the β-pyrrolic positions like bromination, hydroformylation, nitration and chlorosulfonation as well as cycloadditions.[6–14] Reported functionalizations on the *meso*-substituents include S_NAr-reactions[15,16] and Buchwald–Hartwig type Pd-catalyzed aminations.[17] Pd-catalyzed C–C cross-coupling reactions (Suzuki–Miyaura and Liebeskind–Srogl) carried out on metallated (Cu, Mn) corroles have also been reported,[15,16,18] but were limited to *meso*-pyrimidyl substituted corroles and simple boronic acids. Thus, the ability to couple more complex boronic acids with the corrole precursors is of prime importance and would open up a synthetic pathway towards highly functionalized corroles for the already mentioned applications.

In this work, we present the first examples of Suzuki–Miyaura cross-coupling reactions on *meso*-triaryl corroles with heteroaromatic boronic acids and esters, alkenylboronic acids, as well as a highly efficient method for the Suzuki–Miyaura of corroles with simpler boronic acids.

2. Results and discussion

2.1. Synthesis of the A_2B-corrole scaffold and metallation

10-(4-Bromophenyl-)5,15-bis-(pentafluorophenyl)corrole **3**, which was previously synthesized in ionic liquids,[19] was chosen as our basic starting material, since derivatives with pentafluorophenyl-substituents exhibit superior stability than most other compounds

* Corresponding author. Tel.: +43 732 2468 8811; e-mail address: wolfgang.schoefberger@jku.at (W. Schoefberger).

0040-4020/$ – see front matter © 2011 Elsevier Ltd. All rights reserved.
doi:10.1016/j.tet.2011.04.024

with aromatic *meso*-substituents studied to date. The first step in the synthesis of **3** (Scheme 1) was the HCl-catalyzed condensation of pyrrole with pentafluorobenzaldehyde in water/MeOH to give the 5-pentafluorophenyldipyrromethane **2** in 85% yield.[20]

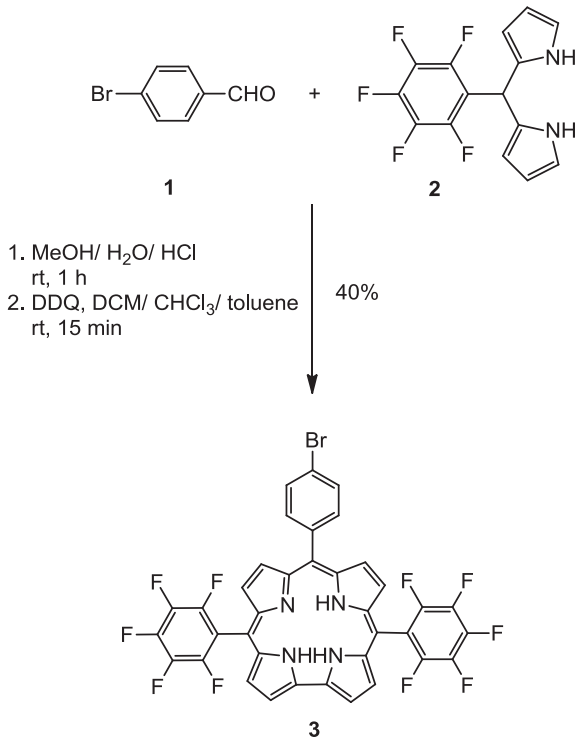

Scheme 1. Synthesis of 10-(4-bromophenyl-)-5,15-bis-(pentafluorophenyl-) corrole **3**.

This step is followed by the condensation of **2** with 4-bromobenzaldehyde in water/MeOH/HCl for 1 h and subsequent oxidation reaction with DDQ,[21] which yields up to 40% of **3**.

The copper-metallation (Scheme 2) was carried out in THF with a threefold excess of Cu(II)acetate and showed almost complete conversion of *meso*-phenyl substituted A_2B-corrole **3** to the Cu(III)-10-(4-bromophenyl-)-5,15-bis-(pentafluorophenyl-)corrole, Cu(III) [(10-(4-BrPh)-5,15-bis-F_5PhC)] **4**.[16]

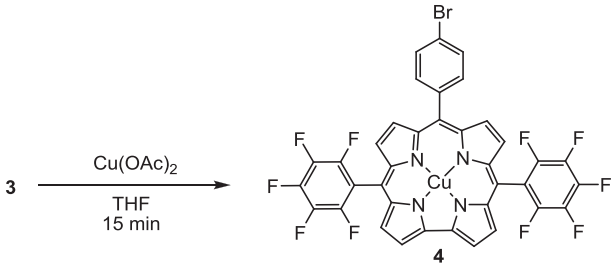

Scheme 2. Cu-metallation of 10-(4-bromophenyl-)-5,15-bis-(pentafluorophenyl-) corrole **4**.

2.2. Suzuki reaction on corroles

Suzuki reaction on corroles was reported earlier,[15,16] but was limited to Cu-metallated *meso*-pyrimidylcorroles. In doubt of the applicability of the classic catalyst system ($Pd(OAc)_2/PPh_3$ or $Pd(0)(PPh_3)_4$, in aqueous medium) on both *meso*-triphenylcorrole derivatives and heterocyclic boronic acids, we searched for a more versatile catalyst system, capable of coupling a large variety of boron derivatives with the corrole system.

Numerous new catalyst systems for Suzuki cross-coupling reactions were reported over the last decade, including NHC-(nitrogen heterocyclic carbene) based Pd-containing systems,[22] Ni-complex based systems[23–25] and new classes of phosphine ligand based catalysts.[26,27] Due to their commercial availability and easy handling we opted for the latter. First attempts with the conditions optimized by Buchwald et al.[26], employing SPhos (2-dicyclohexylphosphino-2′,6′-dimethoxybiphenyl—Scheme 3) asligand, $Pd_2(0)dba_3$ as Pd-containing species (dba=dibenzylideneacetone) and solid K_3PO_4 as base in the absence of water were immediately successful: we were able to couple Cu(III) [(10-(4-BrPh)-5,15-bis-F_5PhC)] **4**, with phenylboronic acid, **6a**, *p*-tolylboronic acid, **6b**, 2-naphthylboronic acid, **6c** and *E*-2-phenylvinylboronic acid, **6d** (Table 1, Scheme 4) with yields up to 84%, whereby no significant formation of side-products was observed.

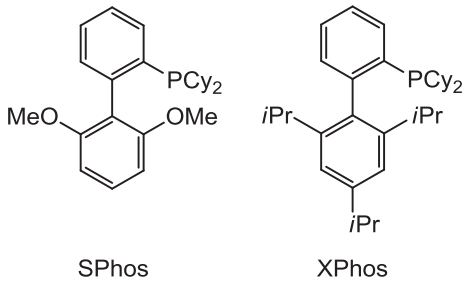

Scheme 3. Phosphane-ligands used in the Suzuki–Miyaura reactions.

At 80 °C, relatively low reaction times were necessary for full conversion of the reactant. As the reaction with neutral and activated aryl boronic acids proved to be more or less unproblematic, we tried to apply the same procedure on unactivated aryl- and heteroaryl boronic acids.

The Suzuki–Miyaura with 2-dimethylaminopyrimidine-5-boronic acid pinacol ester **6e** carried out in toluene/water 10:1 applying the same catalyst system was also successful with 35% yield, although higher reaction times (24 h) were necessary. The reaction of 6-(1-piperazinyl)pyridine-3-boronic acid **6f** went much slower than with the boronic acids used in the previous experiments. After 24 h of a significant amount of a green open-chain side product has formed and could be observed in addition to the non-converted

Table 1
Functionalization of Cu-A_2B-corroles via Suzuki–Miyaura reaction using $Pd_2(dba)_3$ and SPhos[a]

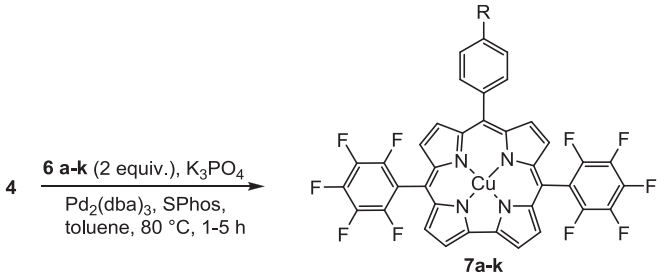

Entry	Boron derivative	Solvent	Temp [°C]	Time [h]	Product	Yield [%]
1	**6a**	Toluene	80	1	**7a**	78
2	**6b**	Toluene	80	5	**7b**	84
3	**6c**	Toluene	80	2	**7c**	84
4	**6d**	Toluene	80	5	**7d**	80
5	**6e**	Toluene/H_2O[b]	80	24	**7e**	35
6	**6k**	Toluene/H_2O[b]	80	24	**7k**	14

[a] Reaction conditions: 1 equiv of **4**, 2 equiv of boron derivative, 3 equiv of K_3PO_4 cat. 10 mol% $Pd_2(dba)_3$ SPhos/Pd=2:1.
[b] Toluene/H_2O 10:1.

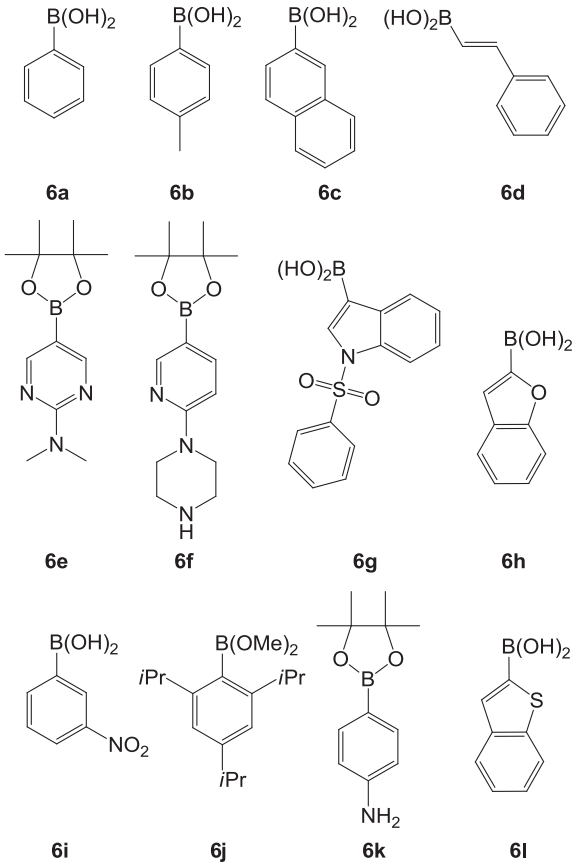

Scheme 4. Boronic acids and boronic acid esters used in the Suzuki couplings with **4**.

reactant and the product. Extending the reaction time to 48 h did just lead to further decomposition of the reactant as well as the product. Furthermore, the reaction with 3-nitrophenylboronic acid, **6i**, 2,4,6-triisopropylphenylboronic acid dimethyl ester, **6j**, and 3-(1-phenylsulfonyl-) indolebronic acid, **6g**, showed absolutely no conversion even after 48 h, when using the SPhos/$Pd_2(dba)_3$ catalyst system. Only the coupling of *p*-amino-phenyl boronic acid pinacol ester **6k** with **4** was achieved, however in very low yields of 14% of **7k**. These results showed the demand of a more efficient catalyst system, which could enable the Suzuki–Miyaura reaction of the corrole system at significantly lower reaction temperatures.

Buchwald et al. recently presented a novel catalyst system **5** (Scheme 5), which is capable of reacting aryl bromides fast and efficient with free boronic acids (reaction scheme, Table 2) at room temperature or 40 °C and in short reaction times of 30 min to 2 h.[27] Precatalyst **5** is easily obtained in a one-pot procedure by combining $Pd(OAc)_2$ with 2-aminobiphenyl, followed by addition of LiCl and the phosphine ligand (XPhos, Scheme 3). We obtained the first crystal structure of the precatalyst **5**. The crystallographic data are summarized in Table S1 (Supplementary data) and the structure is shown in Fig. 1. The crystal structure is published in the Cambridge Crystallographic Data Center with the CCDC number: 813705.

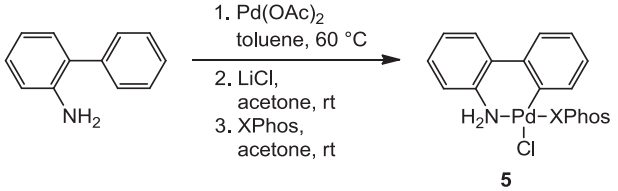

Scheme 5. Synthesis of precatalyst **5**.

Table 2
Functionalization of Cu-A_2B-corroles via Suzuki–Miyaura reaction using Precatalyst **5**[a]

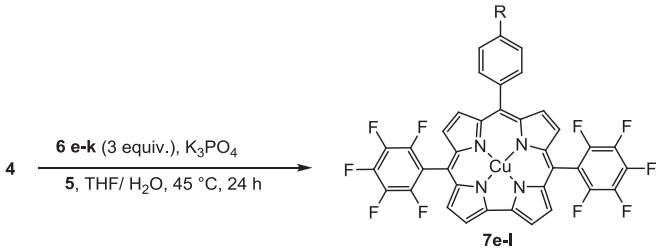

Entry	Boron derivative	Solvent	Temp [°C]	Time [h]	Product	Yield [%]
1	**6e**	THF/H_2O[b]	45	24	**7e**	68
2	**6f**	THF/H_2O[b]	45	24	**7f**	84
3	**6g**	THF/H_2O[b]	45	24	**7g**	72
4	**6h**	THF/H_2O[b]	45	24	**7h**	82
5	**6i**	THF/H_2O[b]	45	24	**7i**	79
6	**6j**	THF/H_2O[b]	45	24	**7j**	—
7	**6k**	THF/H_2O[b]	45	24	**7k**	23
8	**6l**	THF/H_2O[b]	45	24	**7l**	45

[a] Reaction conditions: 1 equiv of **4**, 3 equiv of boronic acid/ester derivative, 3 equiv of K_3PO_4, 10 mol % of **5**.
[b] THF/H_2O 5:3.

The cyclometallated complex **5** generates the catalytically active XPhosPd(0) species quickly under mild conditions under, which the deboronation of the boronic acid derivatives is significantly slowed down, thereby allowing the coupling of less stable boronic acids.

Along with the change of the catalyst system, also the reaction conditions were optimized: the solvent was changed from toluene or toluene/water 10:1 (for boronic acid esters) to THF/water 5:3, and the excess of the boron derivative was increased (from two- to threefold). These alterations induced a significant change in the electronic structure of the copper corrole system: upon the addition of the solvent mixture and the base, the formal oxidation state of the central Cu ion seems to change from copper(III) to copper(II), which was indicated by a conspicuous colour change from brownish-red to green in solution. This finding is supported by UV/vis and NMR experiments, which will be discussed further below.

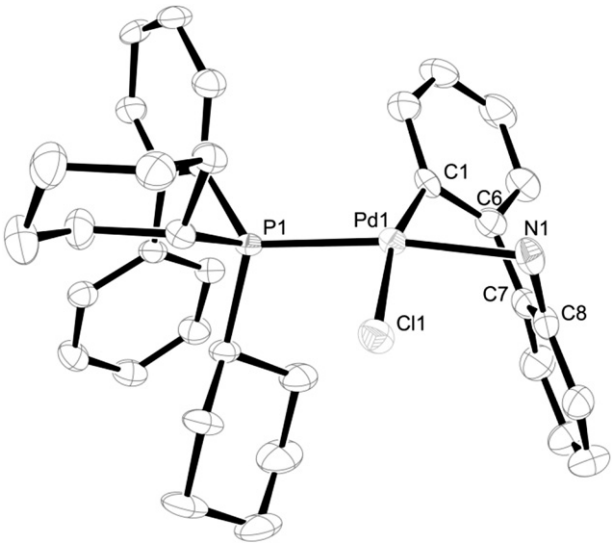

Fig. 1. Molecular structure of **5** (ORTEP displacement ellipsoids at the 50% probability level, H atoms and *i*-Pr substituents are omitted for clarity). Selected bond lengths [Å] and angles [°]: Pd1–C1 2.022 (4), Pd1–P1 2.270 (1), Pd1–Cl1 2.428 (1), Pd1–N1 2.119 (3), C1–Pd1–N1 82.9 (1), C1–Pd1–P1 98.6 (1), Cl1–Pd1–N1 86.1 (1), Cl1–Pd1–P1 91.62 (3).

Applying the improved catalyst system as well as the altered reaction conditions, the heterocyclic boronic acids and boronic acid pinacolesters **6e**–**h** could be efficiently coupled with the corrole **4** within 24 h at 45 °C (Table 2).

More precisely, the Suzuki–Miyaura reaction with 2-dimethylamino-pyrimidyl-5-boronic acid pinacol ester, **6e**, 6-(piperazin-1-yl) pyridine-3-boronic acid pinacol ester, **6f**, 1-(phenylsulfonyl)indole-3-boronic acid, **6g**, 2-benzofuranboronic acid, **6h** gave product yields of **7e**–**h** higher than 70% (Table 2) though product **7f** was not permanently stable. Its degradation was observed immediately after a second column chromatographic purification step. Nevertheless, mass spectrometry and UV/vis absorption spectroscopy indicated the formation of the expected compound.

In contrast to the failed coupling attempts with **6i**–**k** described above, the Suzuki–Miyaura reaction of Cu(III) [(10-(4-BrPh)-5,15-bis-F_5PhC)], **4**, with 3-nitrophenylboronic acid **6i**, and *p*-aminophenyl boronic acid pinacol ester **6k** now gave overall yields of about 79% and 23%, respectively. A possible side reaction in case of **6k** is the Buchwald–Hartwig reaction of the amino-group with **4** via an N–C-coupling reaction.[28–30] The Suzuki–Miyaura reaction of **4** with 2-benzo[*b*]thiopheneboronic acid **6l** under described conditions exhibited an average yield of 45% of product **7l**.

2.3. Cu(III) corrole versus Cu(II) corrole species

In the absence of other ligands, the formal oxidation state of copper corroles corresponds to a diamagnetic Cu^{3+} (d^8) center, bound to a trianionic corrolate macrocycle. In practice, the presence of polar covalent bonds and the possibility of back-bonding between the corrolate π-electron system and the (formally empty) Cu $3d_{x^2-y^2}$ orbital gives rise to a much smaller effective charge at the copper center. Such an electron donation may be accomplished by two alternative interaction types: (a) a dative bond from the corrolate nitrogen lone pairs to the Cu^{+3} ion, providing a more covalent character to the copper-corrolate σ-bonds, (b) transfer of electron density from the corrolate trianion into the empty $3d_{x^2-y^2}$ orbital via σ–π interactions induced by a saddling deformation of the macrocycle. In the latter case, the Cu(III)-corrolate^{3-} system is in equilibrium with a d^9-species with Cu(II)corrolate$^{\bullet 2-}$ radical character, which can adopt either an antiferromagnetically coupled singlet state (saddle-shape geometry) or a planar triplet state.[31–38] The well resolved ^{1}H NMR spectrum observed in dichloromethane at 283 K (Fig. 2A) reflects, that the equilibrium for the copper A_2B-corrole **3** lies on the side of a diamagnetic species where almost no charge redistribution between the corrole ligand π-orbitals and the $3d_{x^2-y^2}$ orbital occurs.

In alkaline THF/H_2O/K_3PO_4 media the equilibrium is shifted towards the Cu(II)-corrolate$^{\bullet 2-}$ dianion radical species best seen by the vanished pyrrole proton resonances and the increased line broadening of the proton resonances stemming from the phenyl moiety. All proton spin systems therefore possess faster relaxation rates caused by the increased paramagnetic property of the central copper ion. Clearly, the pyrrole proton resonances are most sensitive, due to the close proximity of the pyrrole protons to the paramagnetic copper central atom. Furthermore, an ESR signal was observed at room temperature in dichloromethane (Supplementary data—Fig. 52). Complementary, the UV/vis absorption spectra of [Cu^{III}(10-Br-Ph-5,15-bis-F_5PhC)], **4**, illustrated in Fig. 2B, exhibit a bathochromic shift of the Soret-band maximum from 407 to 433 nm after the addition of aq K_3PO_4 solution. A similar trend was published earlier, by employing spectroelectrochemical and ESR studies on similar highly substituted copper A_3-corroles.[39] All those findings could not be observed in toluene/H_2O/K_3PO_4. Hence, we hypothesize that in THF/H_2O/K_3PO_4 mixture (water and solvent miscible) preferably the Cu(II)-corrolate$^{\bullet 2-}$ diradical species is existent, whereas in toluene/H_2O/K_3PO_4 the reactant dominates in the Cu(III) form.

Furthermore, the increased Cu(II) character of the central metal ion is observed in reaction products **7a**–**d** indicated by a more intense electronic transition at 433 nm in the UV/vis spectra (Fig. 3A) and an increased line-width in the ^{1}H NMR experiments. In compound **4**, the diamagnetic Cu(III) oxidation state is stabilized, whereas aromatic moieties in **7a**–**e** shift the equilibrium more or less towards the Cu(II) species (indicated by an increasing shoulder at 433 nm). Fig. 3B shows the ESR-spectrum observed for **7a** in dichloromethane at 298 K. The ESR spectrum of compound **7a** exhibits unsymmetrical four lines at g=2.077 with hyperfine splitting due to the Cu nucleus (I=3/2). In the Supplementary data (Fig. 52) we have additionally attached ESR spectrum of **7a** in dichloromethane solution at 1.5 K.

2.4. Density functional theory (DFT) and time-dependent DFT (TD-DFT) calculations

Geometry optimization of Cu(III) [(10 (4-BrPh) 5,15 bisF_5PhC)] **7a** indeed also results in a saddled-shape distorted structure (Fig. 4B) and the obtained molecular structure is almost identical to the crystal structure of **7a** depicted in Fig. 4A.

The similarity of both crystal structure and calculated structure appears when opposing the N–Cu–N angles of both structures.

Experimentally observed angles are 82.0°, 91.6°, 91.0° and 97.3° for the compound **7a** and match closely to the calculated ones 81.8°, 91.5°, 91.2° and 97.0°. Consequently, also the corresponding Cu–N-distances match pretty well. (Experiment: Cu1–N1 1.876, Cu1–N2 1.880, Cu1–N3 1.892, Cu1–N4 1.891, calculations: 1.881 Å, 1881 Å, 1.903 Å, 1.904 Å). Furthermore, the enhanced saddling distortion of the corrole backbone in **7a**, measured as the mean angle between planes (χ) of opposite pyrrole rings are experimentally determined to be χ=15.4° and χ=17.3°. The corresponding calculated χ-angles are 15.1° and 17.1°.

The conformation of the corrole ligand however rearranges from the saddle-shape structure to a more relaxed geometry when applying the geometry optimization on the Cu(III) [(10 (4-BrPh) 5,15 bisF_5PhC)] (Fig. 4C). Subsequent time-dependent density functional theoretical calculations on both species support the experimentally observed UV/vis spectra (performed in THF/H_2O) reasonably well (Fig. 4D, E). Fig. 4D exhibits the characteristic spectrum of the Cu(III) corrole **7a** with a B band (Soret Band) maximum of 405 nm and a broader Q-band region around 550 nm. By comparing the results obtain from the calculations both spectral features (B- and Q-bands) could be reproduced and moreover the bathochromic shift of about Δλ=30 nm is also consistent to spectroelectrochemical data obtained for the first reduction,[39] when calculating the corresponding reduced Cu(II)–corrole moiety (Fig. 4E). Even the spectral features are consistent, observable by the emerging shoulder in the B-band region ($\lambda_{max,calcd}$=435 nm and λ_{exp}=433 nm) and a more defined Q-band emerging at λ_{calcd}=570 nm versus λ_{exp}=590 nm. The electronic transitions are further described in the electronic Supplementary data (Fig. 47–51).

3. Conclusion

In summary, we have developed a procedure for Suzuki–Miyaura reactions at 80 °C with a SPhos/$Pd_2(dba)_3$ catalyst system and a milder synthesis routine at 45 °C with a Pd-precatalyst system, that allows the coupling of corrole bromides with a wide range of boronic acid/ester derivatives and exhibits excellent functional group tolerance. Moreover, the fast catalytic process of the latter catalyst system **5** at lower temperature offers an excellent way to couple heterocyclic boronic acids with corrole bromides.

Depending on the solvents used in the Suzuki–Miyaura reaction, a bathochromic shift in UV/vis absorption spectra and increased line broadening of proton resonances in the ^{1}H NMR

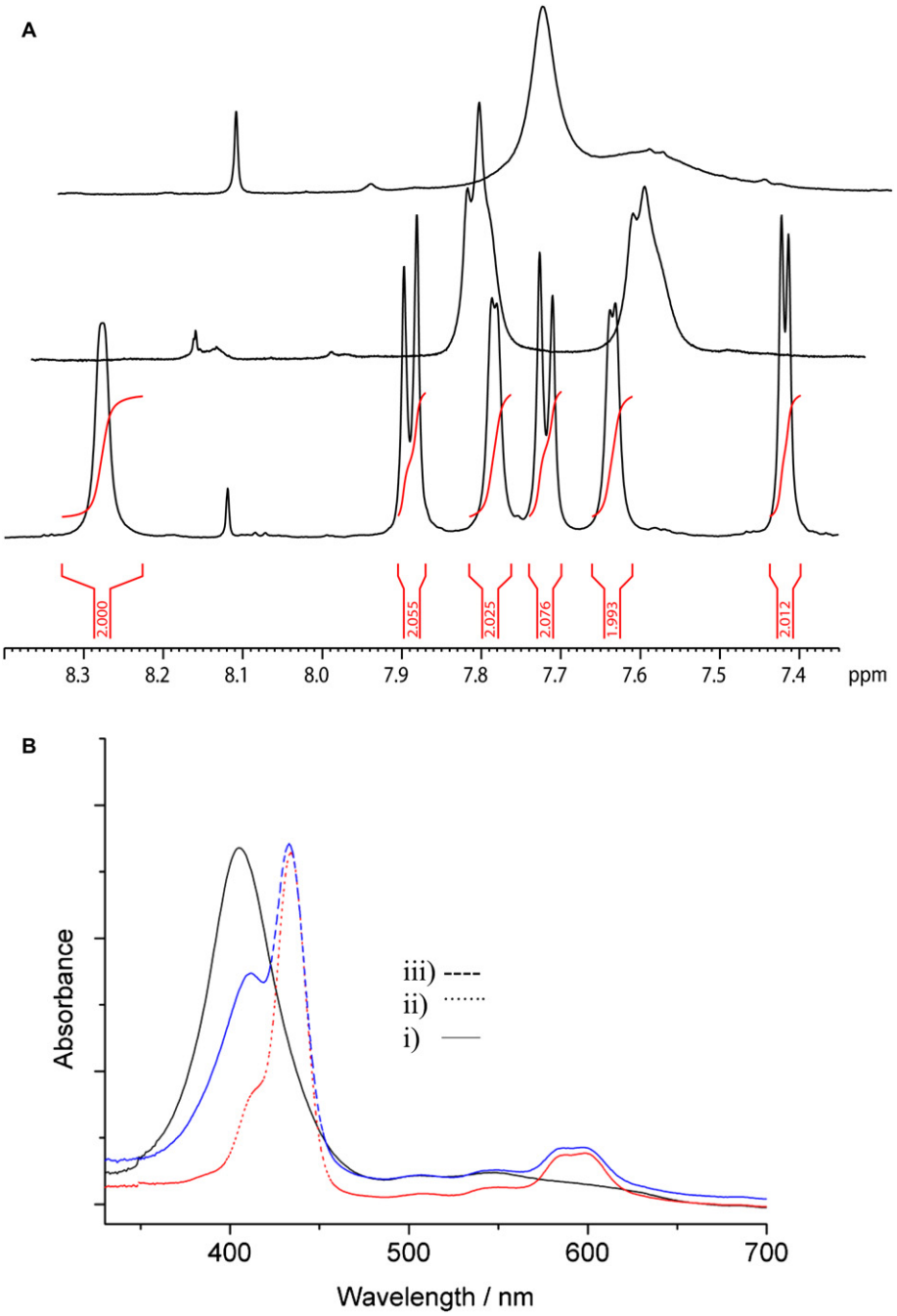

Fig. 2. A. Time-course ^{1}H NMR spectra and B. UV/vis spectra of the reduction process of Cu(III) corrole aryl bromide **3** in pure (i) THF-d_8 (ii) in a mixture of THF-d_8/D_2O and (iii) in a mixture of THF-d8/D_2O/K_3PO_4.

spectra of the copper-[(10-(4-BrPh)-5,15-bis-F_5PhC)] corrole complexes was observed. Therefore, the formal oxidation state of copper is not self-evident in all cases and has to be clarified by further investigations.

Most of the Suzuki–Miyaura coupled products form stable Cu(III) corroles in solution and in the solid state. Activating substituents however, like phenyl- or pyrimdyl-groups lead to coupled products exhibiting significant Cu(II)-character. The DFT geometry optimized structure of **7a** matches well with the crystal structure and TD-DFT approaches support the band-shift observed in UV/vis spectra and moreover indicate a conformational change from a saddled Cu(III) corrole species with Cu–N distances of d_{Cu-N}=1.88–1.89 Å to a more relaxed geometry of the corresponding Cu(II) corrole with calculated Cu–N distances of d_{Cu-N}=1.92–1.93 Å.

4. Experimental section

4.1. General experimental

All chemicals were purchased from Sigma–Aldrich or Acros and used without further purification. Reagent grade solvents were purchased from Fischer chemicals and distilled prior to use. THF was distilled over sodium and benzophenone under an argon atmosphere and toluene was distilled over sodium/potassium alloy and benzophenone under an argon atmosphere and was stored over molecular sieves (4 Å) upon use. Acetone (HPLC-grade) was stored over molecular sieves (3 Å) upon use.

Proton (^{1}H NMR) and carbon (^{13}C NMR) spectra were recorded on Bruker DRX 500 spectrometer equipped with a cryogenically

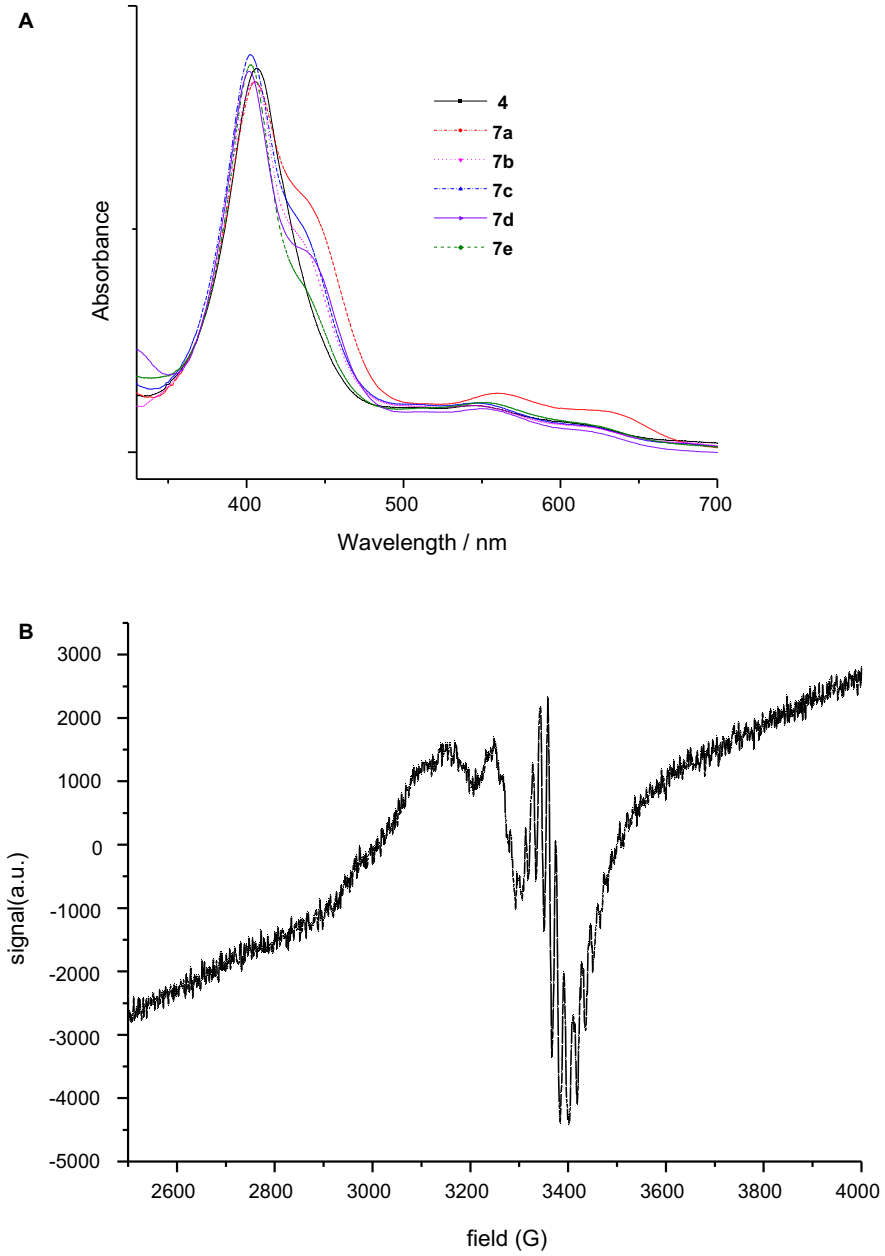

Fig. 3. A. UV/vis spectra of **4** as reference Cu(III) corrole species and the compounds **7a**–**e** exhibiting increased Cu(II) character in dichloromethane solution. B. ESR spectrum of **7a** in dichloromethane solution at 298 K.

cooled probe (TXI) at 500 and 125.8, respectively, ^{19}F NMR spectra were recorded on a Bruker AV 600 MHz or a Varian Inova 300 MHz spectrometer at 564.7 and 282.4 MHz, respectively, and phosphorus (^{31}P NMR) NMR spectra were recorded on a Bruker 200 MHz spectrometer at 80.9 MHz.

The chemical shifts are given in parts per million (ppm) on the delta scale (δ) and are referenced to TMS (δ=0 ppm) for ^{1}H, 65% aq H_3PO_4 (δ=0 ppm) for ^{31}P and TFA for ^{19}F. Abbreviations for NMR data: s=singlet, d=doublet, t=triplet, q=quartet, dd=doublet of doublets, dt=doublet of triplets, dq=doublet of quartets, tt=triplet of triplets, m=multiplet. Mass spectra were collected on a Finnigan LCQ DecaXPplus Ion trap Mass spectrometer with ESI ion source and MALDI-TOF measurements were collected with a Bruker Autoflex III Smartbeam spectrometer, whereby a matrix:sample ratio of 10:1 was used.

TLC was performed by using Fluka silica gel 60 F_{254} (0.2 mm) on aluminium plates. Silica-gel columns for chromatography were prepared with E. Merck silica gel 60 (0.063–0.20 mesh ASTM).

4.2. Synthesis of the Fb-A_2B-corrole precursor (3)

Synthesis according to the procedure of Gryko and Koszarna[40]1.281 g (4.1 mmol, 2 equiv) of **2** and 412 mg (2.2 mmol, 1 equiv) of **1** were dissolved in 200 ml of methanol. Subsequently, a solution of 10 ml concentrated HCl in 200 ml of water was added. This suspension was stirred at room temperature (rt) for 1 h and extracted with $CHCl_3$ (2× 50 ml). The combined organic phases were washed with water (3× 50 ml), dried over Na_2SO_4 and concentrated to 40 ml. This solution and a solution of 1.2 g of DDQ (5.3 mmol, 2.5 equiv) in 32 ml DCM/toluene (3:1) were

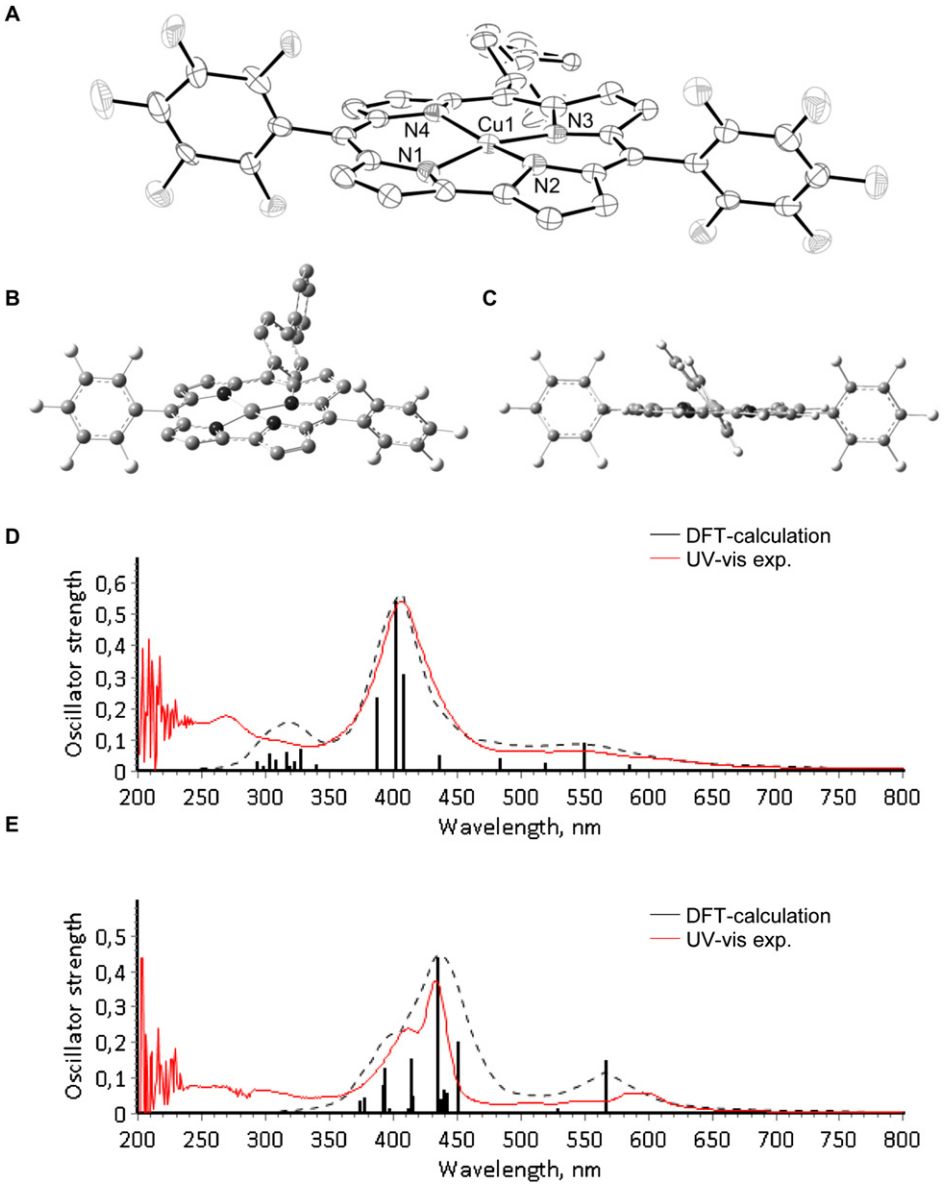

Fig. 4. A. Molecular structure of one of the two independent Cu-corrole molecules in crystals of **7a** (ORTEP, displacement ellipsoids at the 30% probability level, H atoms are omitted for clarity). Selected bond lengths [Å] and angles [°]: Cu1–N1 1.876 (5), Cu1–N2 1.880 (5), Cu1–N3 1.892 (5), Cu1–N4 1.891 (5), N1–Cu1–N2 82.0 (2), N1–Cu1–N4 91.6 (2), N2–Cu1–N3 91.0 (2), N3–Cu1–N4 97.3 (2). The corresponding distances [Å] and angles [°] for the second complex are: Cu2–N5 1.900 (4), Cu2–N6 1.896 (4), Cu2–N7 1.887 (5), Cu2–N8 1.909 (5), N5–Cu2–N6 91.7 (2), N5–Cu2–N8 96.9 (2), N6–Cu2–N7 81.4 (2), N7–Cu2–N8 91.9 (2) B. Ground state DFT-optimized structures of Cu(III) corrole **7a** and C. The corresponding Cu(II) corrole species. D. Experimentally (solid, red line) observed and calculated (dashed, black line) UV/vis spectra of Cu(III) corrole **7a** and the E. the corresponding experimentally (solid, red line) observed and calculated (dashed, black line) electronic transition spectra of the Cu(II) corrole analogue.

simultaneously added to 40 ml vigorously stirred DCM. The reaction mixture was stirred for 15 min at room temperature, concentrated to ¼ of the initial volume and chromatographed (silica, $CHCl_3$/hexanes 1:1). The fluorescent bands were collected and evaporated to dryness. 698 mg (0.88 mmol, 40%). ^{1}H NMR (200 MHz, $CDCl_3$, 30 °C): δ=9.12 (d, J(H,H)=4 Hz, 2H, H$_\beta$), 8.695 (m, 4H, H$_\beta$) 8.57 (d, J(H,H)=4 Hz, 2H, H$_\beta$), 8.05 (d, J(H,H)=7 Hz, 2H, H$_o$), 7.91 (d, J(H,H)=7 Hz, 2H, H$_m$); MS (ESI$^+$): m/z: calcd for $C_{37}H_{15}BrF_{10}N_7$: 784.03; found: 785.08 $[M+H]^+$; UV/vis ($CHCl_3$) λ_{max}=408, 561, 608 nm. Other analytical data were consistent with literature values.[19]

4.3. Cu-metallation reaction (4)

Synthesis according to the procedure of Maes et al.[16] 698.2 mg (0.89 mmol, 1 equiv) of **3** were dissolved in 130 ml THF and this solution was purged with nitrogen for 10 min. 502 mg (2.8 mmol, 3 equiv) of anhydrous copper(II)acetate were placed into a Schlenk tube, followed by the addition of the corrole/THF solution under nitrogen counter flow. This mixture was stirred for 15 min at room temperature under nitrogen atmosphere evaporated to dryness and redissolved in 100 ml DCM. This solution was washed three times with 30 ml water. Evaporation to dryness afforded 687.9 mg (0.81 mmol, 91% yield) of the pure product (purple solid). ^{1}H NMR (600 MHz, CD_2Cl_2, 25 °C): δ=8.02 (s, 2H, H$_\beta$), 7.65 (d, J(H,H)=8 Hz, 2H, H$_o$), 7.45 (m, 4H, H$_m$, H$_\beta$), 7.26 (d, J(H,H)=4 Hz, 2H, H$_\beta$), 7.20 (d, J(H,H)=4 Hz, 2H, H$_\beta$); ^{13}C NMR (125.8 MHz, CD_2Cl_2, 25 °C): δ=131.7 (CH), 131.4 (CH), 130.2 (CH), 125.9 (CH), 125.1 (CH), 122.8 (CH); ^{19}F NMR (564.7 MHz, CD_2Cl_2, 25 °C): δ=−138.03 (s, 4F, F$_o$), −153.33 (d, ^3J(F,F)=20 Hz, 2F, F$_p$), −161.73 (m, 4F, F$_m$); MS (ESI$^-$): m/z: calcd for $C_{37}H_{15}BrCuF_{10}N_7$: 845.94; found: 846.20 $[M]^-$; UV/vis ($CHCl_3$) λ_{max}=406, 548, 617 nm.

4.4. Synthesis of precatalyst 5

Synthesis in analogy to[27] under N_2 atmosphere, 1 mmol $Pd(OAc)_2$ and 1.04 mmol 2-amino-biphenyl were dissolved in 6 ml anhydrous toluene, heated to 60 °C and stirred for 60 min, whereby the solution turned from red to yellowish grey and a grey precipitate formed. Further on, the toluene was removed via cannula and the solution was cooled to ambient temperature. The residue was washed with toluene, and 6 ml acetone and 3 mmol LiCl were added and the solution slowly turned olive green. After 60 min of stirring, 0.95 mmol XPhos were added in five portions and the solution was stirred for further 120 min, during which a grayish white solid precipitated. After a major amount of the solvent was removed via cannula, 1.5 ml MTBE and 3 ml pentane were added. The solution was cooled to 0 °C and after 60 min the product was collected by filtration and washed with water. Yield: 520 mg (66%). ^{31}P NMR (80.9 MHz, $CDCl_3$, 30 °C): δ=67.9, 65.6 ppm (two signals due to two different rotamers); MS (ESI^+): *m/z*: calcd for $C_{45}H_{59}NPPdCl$: 785.31; found: 750.40 $[M-Cl^-]^+$; 582.40 $[M-C_{15}H_{23}]^+$ ^{1}H NMR complex but consistent with literature.[4] Crystal structure is available (CSDC: 813705 and 813706).

4.5. General procedure for the Suzuki-reaction with alkyl and alkenylboronic acids- and boronic acid esters using SPhos and $Pd_2(dba)_3$ as catalyst system

Compound **4** 0.1 mmol (1 equiv), 0.2 mmol (2 equiv) of the corresponding boronic acid, 63.7 mg (0.3 mmol, 3 equiv) of K_3PO_4, 2.3 mg of $Pd_2(0)dba_3$ (5 mol-% Pd) and 2.0 mg of SPhos (ligand to metal ratio 2:1) were filled in a Schlenk-tube, which was sealed with a Teflon cap. The tube was evacuated and backfilled with nitrogen (this process was repeated two times), followed by the addition of 32 ml of toluene (29.1 ml toluene and 2.9 ml water for boronic acid esters) under nitrogen counter flow. The Schlenk-tube was sealed again, and the resulting mixture was stirred for 1–24 h at 80 °C under nitrogen atmosphere. After the completion of the reaction (TLC monitoring), the reaction mixture was suction filtered over a Celite plug (1 cm), the filtrate was evaporated to dryness The residue was dissolved in 30 ml DCM, washed with 10 ml of water (three times), the organic phase was dried over anhydrous Na_2SO_4, evaporated to dryness and purified via column chromatography (silica/varying eluents).

4.6. General procedure for the Suzuki cross-coupling reaction with heteroaromatic boronic acids and boronic acid esters employing precatalyst 5

Compound **4** 0.05 mmol (1 equiv) and 0.15 mmol K_3PO_4 were placed in a Schlenk tube and dissolved in 16 ml of a degassed THF/H_2O mixture (5:3). The solution was purged with N_2 for further 30 min, followed by the addition of 0.15 mmol of the corresponding boronic acid (or ester, respectively) and 10 mol % of precatalyst **5**. The Schlenk tube was sealed, and the reaction mixture was heated to 45 °C and stirred for 24 h (unless not denoted differently for the specific reaction) under N_2. After completion (TLC and ESI-MS monitoring), the reaction mixture was evaporated to dryness, the residue was dissolved in 30 ml of $CHCl_3$ and washed twice with 10 ml of water. The organic phase was then dried over anhydrous Na_2SO_4, evaporated to dryness and purified via column chromatography (silica/varying eluents).

*4.6.1. Compound **7a**: Cu 10-(4,1′-biphenyl-1-yl)5,15-bispentafluorophenylcorrole.* Eluent hexanes/DCM 2:1. 66 mg (78% yield). ^{1}H NMR (500 MHz, CD_2Cl_2, 25 °C): δ=8.01 (d, *J*(H,H)=4 Hz, 2H, H_β), 7.75 (d, *J*(H,H)=8 Hz, 2H, H_o), 7.71 (d, *J*(H,H)=8 Hz, 2H, H_m), 7.66 (d, *J*(H,H)=8 Hz, 2H, H_o), 7.49 (m, 2H, H_m), 7.46 (d, *J*(H,H)=4 Hz, 2H, H_β), 7.40 (m, 1H, H_p), 7.32 (d, *J*(H,H)=4 Hz, 2H, H_β), 7.26 ppm (d, *J*(H,H)=4 Hz, 2H, H_β); ^{13}C NMR (125.8 MHz, CD_2Cl_2, 25 °C): δ=133.8 (CH), 132.6 (CH), 131.5 (CH), 130.3 (CH), 129.3 (CH), 128.5 (CH), 128.3 (CH), 127.8 (CH), 124.4 ppm (CH); ^{19}F NMR (282.4 MHz, CD_2Cl_2, 25 °C): δ=−138.09 (dd, ^3J(F,F)=20 Hz, ^4J(F,F)=8 Hz, 4F, F_o), −153.48 (t, ^3J(F,F)=20 Hz, 2F, F_p), −161.79 ppm (dt, ^3J(F,F)=20 Hz, ^4J(F,F)=8 Hz, 4F, F_m); MS (ESI^-): *m/z*: calcd for $C_{43}H_{17}CuF_{10}N_4$: 842.06; found: 842.07 $[M]^-$. UV/vis (CH_2Cl_2) λ_{max}=401, 557, 623 nm.

*4.6.2. Compound **7b**: Cu 10-(4-(4-methylphenyl-)phenyl-)5,15-bispentafluorophenylcorrole.* Eluent hexanes/DCM 2:1. 72 mg (84% yield). ^{1}H NMR (500 MHz, CD_2Cl_2, 25 °C): δ=8.01 (s, 2H, H_β), 7.7 (d, *J*(H,H)=8 Hz, 2H, H_o), 7.66 (d, *J*(H,H)=8 Hz, 2H, H_m), 7.61 (d, *J*(H,H)=8 Hz, 2H, H_o), 7.47 (m, 4H), 7.32 (m, 4H); 2.42 ppm (s, 3H, H_{Me}); ^{13}C NMR (125.8 MHz, CD_2Cl_2, 25 °C): δ=133.1 (CH), 131.9 (CH), 130.4 (CH), 130.1 (CH), 127.3 (CH), 127.2 (CH), 127.0 (CH), 123.5 (CH), 21.4 (CH_3); ^{19}F NMR (564.7 MHz, CD_2Cl_2, 25 °C): δ=−138.06 (d, ^3J(F,F)=20 Hz, 4F, F_o), −153.48 (m, 2F, F_p), −161.79 ppm (t, ^3J(F,F)=20 Hz, 4F, F_m); MS (ESI^-): *m/z*: calcd for $C_{44}H_{19}CuF_{10}N_4$: 856.07; found: 856.40 $[M]^-$. UV/vis (CH_2Cl_2) λ_{max}=404, 436 (sh), 554, 619 nm.

*4.6.3. Compound **7c**: Cu 10-(4-(2-naphthyl-)phenyl-)5,15-bispentafluorophenylcorrole.* Eluent hexanes/DCM 2:1. 75 mg (84% yield). ^{1}H NMR (500 MHz, CD_2Cl_2, 30 °C): δ=8.20 (s, 1H, H_{naphth}), 7.99 (m, 4H), 7.90 (m, 4H), 7.74 (d, *J*(H,H)=8 Hz, 2H, H_m), 7.53 (m, 2H, H_{naphth}), 7.48 (d, *J*(H,H)=4 Hz, 2H, H_β), 7.375 (d, *J*(H,H)=4 Hz, 2H, H_β), 7.295 (d, *J*(H,H)=4 Hz, 2H, H_β); ^{13}C NMR (125.8 MHz, CD_2Cl_2, 30 °C): δ=133.5 (CH), 132.2 (CH), 131.1 (CH), 129.5 (CH), 128.4 (CH), 127.5 (CH), 127.4 (CH), 126.9 (CH), 126.3 (CH), 126.2 (CH), 124.0 (CH); ^{19}F NMR (564.7 MHz, CD_2Cl_2, 30 °C): δ=−138.02 (d, ^3J(F,F)=20 Hz, 4F, F_o), −153.43 (t, ^3J(F,F)=20 Hz, 2F, F_p), −161.77 ppm (t, ^3J(F,F)=20 Hz, 4F, F_m); MS (ESI^-): *m/z*: calcd for $C_{47}H_{19}CuF_{10}N_4$: 892.07; found: 892.40 $[M]^-$; UV/vis (CH_2Cl_2) λ_{max}=400, 437 (sh), 545, 611 nm.

*4.6.4. Compound **7d**: Cu 10-(4-(E-phenylvinyl-)phenyl-)5,15-bispentafluorophenylcorrole.* Eluent hexanes/DCM 2:1. 70 mg (80% yield). ^{1}H NMR (500 MHz, CD_2Cl_2, 25 °C): δ=8.01 (s, 2H, H_β), 7.60 (d, *J*(H,H)=7 Hz, 2H, H_o), 7.59 (m, 4H), 7.47 (m, 2H, H_β), 7.40 (t, *J*(H,H)=7 Hz, 2H, H_m), 7.26 ppm (m, 7H); ^{13}C NMR (125.8 MHz, CD_2Cl_2, 25 °C): δ=136.1 (CH), 134.9 (CH), 134.0 (CH), 133.9 (CH), 133.2 (CH), 133.2 (CH), 132.5 (CH), 131.0 (CH), 130.7 (CH), 129.5 (CH), 127.6 ppm (CH); ^{19}F NMR (564.7 MHz, CD_2Cl_2, 30 °C): δ=−138.03 (^3J(F,F)=19 Hz, 4F, F_o), −153.42 (t, ^3J(F,F)=19 Hz, 2F, F_p), −161.76 ppm (t, ^3J(F,F)=19 Hz, 4F, F_m); MS (ESI^-): *m/z*: calcd for $C_{45}H_{19}CuF_{10}N_4$: 868.07; found: 868.33 $[M]^-$; UV/vis (CH_2Cl_2) λ_{max}=402, 436 (sh), 550, 616 nm. Product contains an amount of *Z*-isomer.

*4.6.5. Compound **7e**: Cu 10-(4-(2-dimethylaminopyrimidine-5-yl-)phenyl-)5,15-bispentafluorophenylcorrole.* Eluent DCM/MeOH 200:1. 30 mg (68% yield). ^{1}H NMR (500 MHz, CD_2Cl_2, 10 °C): δ=8.66 (s, 2H, H_{pyrim}), 7.96 (s, 2H, H_β), 7.69 (d, *J*(H,H)=7 Hz, 2H, H_o), 7.62 (d, *J*(H,H)=7 Hz, 2H, H_m), 7.49 (s, 2H, H_β), 7.325 (d, *J*(H,H)=4 Hz, 2H, H_β), 7.24 (s, 2H, H_β), 3.22 ppm (s, 6H, H_{methyl}) ^{13}C NMR (125.8 MHz, CD_2Cl_2, 10 °C): δ=156.9 (CH), 132.8 (CH), 131.9 (CH), 130.7 (CH), 126.3 (CH), 126.2 (CH), 124.2 (CH), 38.1 (CH_3); ^{19}F NMR (564.7 MHz, CD_2Cl_2, 30 °C): δ=−138.05 (d, ^3J(F,F)=20 Hz, 4F, F_o), −153.39 (t, ^3J(F,F)=20 Hz, 2F, F_p), −161.74 ppm (t, ^3J(F,F)=20 Hz, 4F, F_m); MS (ESI^+): *m/z*: calcd for $C_{43}H_{20}CuF_{10}N_7$: 887.09; found: 888.33 $[M+H]^+$; MS (ESI^-): *m/z*: calcd for $C_{43}H_{20}CuF_{10}N_7$: 887.09; found: 887.40 $[M]^-$; UV/vis (CH_2Cl_2) λ_{max}=403, 551, 623 nm.

*4.6.6. Compound **7f**: Cu 10-(4-(6-(1-piperazinyl-)pyridine-3-yl-)phenyl-)5,15-bispentafluorophenylcorrole.* Eluent $CHCl_3$/MeOH 10:1 with 1% TEA. 39 mg (84% yield). No NMR data could be obtained due to the fast decomposition of the product. MS (ESI^+): *m/z*: calcd for $C_{46}H_{24}CuF_{10}N_7$: 927.12; found: 928.13 $[M+H]^+$; MS (ESI^-): *m/z*: calcd for $C_{46}H_{24}CuF_{10}N_7$: 927.12; found: 927.40 $[M]^-$; UV/vis

($CHCl_3$) λ_{max}=430, 544, 592 nm. The product is very unstable, and both, in solid and solution, partial decomposition and reduction to the corresponding Cu(II) species is observed.

*4.6.7. Compound **7g**: Cu 10-(4-(1-phenylsulfonylindole-3-yl-)phenyl-) 5,15-bispentafluorophenylcorrole.* Eluent hexanes/DCM 2:1. A second column chromatography was necessary (silica, hexanes/DCM 1:1). 37 mg (72% yield). ^{1}H NMR (500 MHz, CD_2Cl_2, 10 °C): δ=8.10 (d, J(H,H)=8.2 Hz, 1H, indolyl-H7), 8.02 (br s, 2H, H_β), 7.98 (d, J(H,H)=7.5 Hz, 2H, phen-sulfonyl H_o), 7,91 (m(overlapping), 1H, indolyl H4), 7.89 (d(overlapping), 2H, phenyl H_m), 7,86 (s(overlapping), 1H, indolyl H2), 7.77 (d, J(H,H)=7.9 Hz, 2H, phenyl H_m), 7.70 (d, J(H,H)=7.9 Hz, 2H, phenyl H_o) 7.57–7.62 (m, 1H, phen-sulfonyl H_p), 7.45 (br s (overlapping), 2H, H_β), 7.40–7.43 (m, 1H, indolyl H5), 7.33–7.37 (m, 1H, indolyl H6), 7.33 (br s, 2H, H_β), 7.28 (br s, 2H, H_β); ^{13}C NMR (125.8 MHz, CD_2Cl_2, 10 °C): δ=132.9 (CH, 2C, C_β), 131.2 (CH, 2C, phenyl C_o), 130.1 (CH, 1C, phen-sulfonyl C_p), 130.8 (CH, 2C, C_β), 129.9 (CH, 2C, C_β), 128.1 (CH, 2C, phenyl Cm), 127.5 (CH, 2C, phen-sulfonyl Co), 127.5 (CH, 2C, phen-sulfonyl Cm), 125.7 (CH, 1C, indolyl C5), 124.5 (CH, 1C, indolyl C6), 123.9 (CH, 2C, C_β), 123.9 (CH, 1C, indolyl C2), 121.0 (CH, 1C, indolyl C4), 114.4 (CH, 1C, indolyl-C7); ^{19}F NMR (282.4 MHz, CD_2Cl_2, 25 °C): δ=−138.02 (dd, ^3J(F,F)=21 Hz), −153.38 (t, ^3J(F,F)=21 Hz, 2F, F_p), −161.74 ppm (dt, ^3J(F,F)=21 Hz, ^4J(F,F)=7.5 Hz, 4F, F_m); MS (ESI^-): m/z: calcd for $C_{51}H_{21}CuF_{10}N_5O_2S$: 1021.06; found: 1021.25 $[M]^-$, 880.23 [M−phenylsulfonyl]$^-$; UV/vis (CH_2Cl_2) λ_{max}=401, 430(sh), 5550, 610 nm.

*4.6.8. Compound **7h**: Cu 10-(4-(benzo[b]furan-2-yl-)phenyl-)5,15-bispentafluorophenylcorrole.* Eluent hexanes/DCM 1:1. 36 mg (82% yield). ^{1}H NMR (500 MHz, CD_2Cl_2, 25 °C): δ=8.00 (br s, 2H, H_β), 7.71 (d, J(H,H)=8.0 Hz, 2H, H_m), 7,65 (d, J(H,H)=7.7 Hz, 1H, Benzofuranyl-H4), 7.57 (d, J(H,H)=7.8 Hz, 1H, Benzofuranyl-H7), 7.48 (d(overlapping), 2H, H_β), 7.45 (m, 1H, Benzofuranyl-H5), 7.36–7.32 (m, 1H, Benzofuranyl-H6), 7.33 (m(overlapping), 2H, H_β), 7.27 (m(overlapping), 2H, H_o), 7.26 (m(overlapping), 2H, H_β), 7.21 (s, 1H, Benzofuranyl-H3); ^{13}C NMR (125.8 MHz, CD_2Cl_2, 25 °C): 131.3 (CH, 2C, C_β), 130.3 (CH, 2C, C_m), 129.5 (CH, 2C, C_β), 125.2 (CH, 2C, C_β), 125.0 (CH, 1C, Benzofuranyl-C5), 124.1 (CH, 1C, Benzofuranyl-C6), 123.2 (CH, 2C, C_β), 122.5 (CH, 2C, C_o), 120.4 (CH, 1C, Benzofuranyl-C4), 110.5 (CH, 1C, Benzofuranyl-C7), 101.5 (CH, 1C, Benzofuranyl-C3); ^{19}F NMR (282.4 MHz, CD_2Cl_2, 25 °C): δ=−138.08 (dd, ^3J(F,F)=21 Hz, ^4J(F,F)=7.8 Hz, 4F, F_o), −153.40 (t, ^3J(F,F)=21 Hz, 2F, F_p), −161.76 ppm (dt, ^3J(F,F)=21 Hz, ^4J(F,F)=7.8 Hz, 4F, F_m); MS (ESI^-): m/z: calcd for $C_{45}H_{17}CuF_{10}N_4O$: 882.05; found: 882.27 $[M]^-$; UV/vis (CH_2Cl_2) λ_{max}=403, 431(sh), 546, 601 nm;

*4.6.9. Compound **7i**: Cu 10-(4-(m-nitro-phenyl)phenyl-)5,15-bispentafluorophenylcorrole.* Eluent hexanes/DCM 2:1. 35 mg (79% yield). ^{1}H NMR (500 MHz, CD_2Cl_2, 10 °C): δ=8.51 (s, 1H, nitrophen-H2′), 8.29 (d, J(H,H)=8.3 Hz, 1H, nitrophen-H4′), 8.22 (br m, 2H, H_β), 8.00 (J(H,H)=8.2 Hz, 1H, nitrophen-H6′), 7.78–7.84 (m, 1H, nitrophenn-H5′), 7.72 (d, J(H,H)=7.5 Hz, 2H, H_m), 7.49 (br s, 2H, H_β), 7.40 (m, 2H, H_o), 7.23 (br s, 2H, H_β), 7.29 (br s, 2H, H_β); ^{13}C NMR (125.8 MHz, CD_2Cl_2, 25 °C): δ=133.4 (CH), 130.6 (CH), 129.5 (CH), 126.2 (CH), 124.5 (CH), 122.4 (CH), 122.0 (CH), 121.3 (CH), 118.5 (CH), 118.2 (CH); ^{19}F NMR (282.4 MHz, CD_2Cl_2, 25 °C): δ=−138.08 (br d, ^3J(F,F)=22 Hz, 4F, F_o), −153.36 (t, ^3J(F,F)=22 Hz, 2F, F_p), −161.79 ppm (bt, ^3J(F,F)=22 Hz, 4F, F_m); MS (MALDI$^+$): m/z: calcd for $C_{43}H_{16}CuF_{10}N_5O_2$: 887.04; found: 887.22 $[M]^+$; UV/vis (CH_2Cl_2) λ_{max}=403, 422(sh), 547, 604 nm;

*4.6.10. Compound **7j**: Cu 10-(4-(2,4,6-tri(isopropyl)-phenyl)phenyl-) 5,15-bispentafluorophenylcorrole.* Only traces of the reaction product were observed in the reaction mixture: MS (MALDI$^+$): m/z: calcd for $C_{52}H_{35}CuF_{10}N_4$: 968.20; found: 968.41 $[M]^+$;

*4.6.11. Compound **7k**: Cu 10-(4-aminophenyl-)5,15-bispentafluorophenylcorrole.* Eluent DCM/hexanes 10:1. 10 mg (23% yield). ^{1}H NMR (500 MHz, CD_2Cl_2, 25 °C): δ=7.97 (s, 2H, H_β), 7.64 (d, J(H,H)=8 Hz, 2H, H_o), 7.59 (d, J(H,H)=8 Hz, 2H, H_m), 7.49 (d, J(H,H)=8 Hz, 2H, H_o), 7.43 (d, J(H,H)=4 Hz, 2H, H_β), 7.31 (d, J(H,H)=4 Hz, 2H, H_β), 7.23 (d, J(H,H)=4 Hz, 2H, H_β), 6.76 (d, J(H,H)=8 Hz, 2H, H_m), 3.83 ppm (s, H, NH_2); ^{13}C NMR (125.8 MHz, CD_2Cl_2, 25 °C): δ=132.8 (CH), 131.3 (CH), 130.2 (CH), 128.1 (CH), 126.7 (CH), 126.1 (CH), 123.2 (CH), 115.4 (CH); ^{19}F NMR (564.7 MHz, CD_2Cl_2, 30 °C): δ=−138.04 (d, ^3J(F,F)=17 Hz, 4F, F_o), −153.39 (t, ^3J(F,F)=19 Hz, 2F, F_p), −161.80 ppm (t, ^3J(F,F)=19 Hz, 4F, F_m); MS (ESI^+): m/z: calcd for $C_{43}H_{18}CuF_{10}N_5$: 857.07; found: 858.07 $[M+H]^+$; MS (ESI^-): m/z: calcd for $C_{43}H_{20}CuF_{10}N_7$: 857.07; found: 857.47 $[M]^-$; UV/vis (CH_2Cl_2) λ_{max}=404, 552, 616 nm.

*4.6.12. Compound **7l**: Cu 10-(4-(4-benzo[b]thiophen-2-yl-)phenyl-) 5,15-bispentafluorophenylcorrole.* Eluent hexanes/DCM 2:1. 20 mg (45% yield). ^{1}H NMR (500 MHz, CD_2Cl_2, 10 °C): δ=8.03 (2H, H_β), 7.88 (2H, H_m), 7.88 (2H, H_β), 7.67 (2H, H_o), 7.72 (s, 1H, Benzothienyl-H3), 7.71 (d, 1H, Benzothienyl-H7), 7.59 (d, J=7.20 Hz, 1H, Benzothienyl-H4), 7.34–7.41 (m, 1H, Benzothienyl-H6), 7.33 (2H, H_β), 7.28 (2H, H_β), 7.13–7.18 (m, 1H, Benzothienyl-H5). ^{13}C NMR (125.8 MHz, CD_2Cl_2, 25 °C): δ=131.7 (CH), 130.6 (CH), 129.3 (CH), 128.4 (CH), 125.2 (CH), 124.0 (CH), 123.9 (CH), 122.2 (CH), 121.8 (CH), 119.5 (CH), 119.3 (CH); ^{19}F NMR (282.4 MHz, CD_2Cl_2, 25 °C): δ=−138.07 (br d, ^3J(F,F)=20 Hz, 4F, F_o), −153.39 (t, ^3J(F,F)=20 Hz, 2F, F_p), −161.77 ppm (m, 4F, F_m); MS (MALDI$^+$): m/z: calcd for $C_{45}H_{17}CuF_{10}N_4S$: 898.03; found: 898.07 $[M]^+$; UV/vis (CH_2Cl_2) λ_{max}=402, 431(sh), 547, 606 nm.

4.7. DFT-calculations

Calculations were performed by using the Gaussian 03 package of programs.[41] The electronic structure calculations were based on the Kohn-Sham density functional theory (KS-DFT) with Becke's three-parameter hybrid functional (B3LYP) and at DFT/mPW1PW91 level.[42,43] Relativistic electronic core potentials (ECPs)[44] were used to describe the electrons of Cu atoms. The basis set of Peterson and Puzzarini[45] was augmented by adding one set of polarization functions on all atoms and one set of diffuse functions on all non-hydrogen atoms. For C and H atoms all-electron split-valence 6-311+G(d,p) basis sets supplemented with a single set of diffuse functions on carbon atoms were employed. The vertical singlet electronic states were studied using the extended Koopman's theorem with time-dependent PBE0 density functional method (TD-PBE0/BS-II).[46] Energies and dipole moments reported herein were evaluated using the second- and fourth-order Moeller-Plesset perturbation theory [MP2(full)/BS-II or MP4(SDQ)/BS-II] in combination with PBE0 parametrization [PBE0/BS-I].

4.8. Crystal structure determination

Crystals of **5** and **7a** were mounted on a Mitegen Micromount were automatically centred on a Bruker SMART X2S benchtop crystallographic system. Intensity measurements were performed using monochromated (doubly curved silicon crystal) Mo Kα-radiation (0.71073 Å) from a sealed microfocus tube. APEX2 software was used for preliminary determination of the unit cell.[47] Determinations of integrated intensities and unit cell refinement were performed using SAINT.[48] Data were corrected for absorption effects with SADABS using the multi-scan technique.[49] The structures were solved by direct methods (SHELXS-97)[51] and refined by full-matrix least-squares on F_0^2 (SHELXL-97).[50,51] The H atoms were calculated geometrically, and a riding model was applied during the refinement process.

The cell parameters of **7a** suggest a monoclinic space group, but the tolyl substituent could not be resolved in $P2_1/c$. Structure solution in the triclinic space group $P-1$ reveals a disorder of the tolyl

and one pentafluorophenyl substituent. The structure was refined with two positions of each disordered aromatic moiety rotated about the C_{ipso}–C_{para} positions. Their site occupancy factors were refined to ~52:48 for both disordered pentafluorophenyl and one phenyl-group and to 55:45 for the other phenyl-moiety. As this disorder model is still not yielding acceptable structural parameters of the disordered groups, the bond distances were fixed with the DFIX command and the rings flattened with FLAT command. All 86 restrains originate form this description of the disorder. Crystals of the precatalyst **5** contain two molecules of chloroform one of which is disordered. Hence, the program SQUEEZE,[52] a part of the PLATON package of crystallographic software, was used to calculate the solvent disorder area and remove its contribution to the overall intensity data.

Acknowledgements

This work was supported by the Austrian Science Fund, projects P-18384 (to W.S.) and the European Community (EU-NMR, contract No. RII 3-026145).

We would like to thank Dr. Manuela List for her support in measuring our samples on the ESI-Q-TOF mass spectrometer.

Supplementary data

Supplementary data associated with this article can be found in the online version at doi:10.1016/j.tet.2011.04.024.

References and notes

1. Gross, Z.; Galili, N.; Saltsman, I. *Angew. Chem.* **1999**, *111*, 1530.
2. Gross, Z.; Galili, N.; Saltsman, I. *Angew. Chem., Int. Ed.* **1999**, *38*, 1427.
3. Gross, Z.; Galili, N.; Simkhovich, L.; Saltsman, I.; Botoshansky, M.; Bläser, D.; Boese, R.; Goldberg, I. *Org. Lett.* **1999**, *1*, 599.
4. Paolesse, R.; Jaquinod, L.; Nurco, D. J.; Mini, S.; Sagone, F.; Boschia, T.; Smith, K. M. *Chem. Commun.* **1999**, 1307.
5. Aviv-Harel, I.; Gross, Z. *Chem.—Eur. J.* **2009**, *15*, 8382.
6. Gryko, D. T. *Eur. J. Org. Chem.* **2002**, 1735.
7. Gryko, D. T.; Fox, J. P.; Goldberg, D. P. *J. Porphyrins Phthalocyanines* **2004**, *8*, 1091.
8. Ghosh, A. *Angew. Chem.* **2004**, *116*, 1952.
9. Ghosh, A. *Angew. Chem., Int. Ed.* **2004**, *43*, 1918.
10. Nardis, S.; Monti, D.; Paolesse, R. 2005, 2, 355.
11. Paolesse, R. *Synlett* **2008**, 2215.
12. Gryko, D. T. *J. Porphyrins Phthalocyanines* **2008**, *12*, 906.
13. Vale, L. S. H. P.; Barata, J. F. B.; Santos, C. I. M.; Neves, M. G. P. M. S.; Faustino, M. A. F.; Tomé, A. C.; Silva, A. M. S.; Paz, F. A. A.; Cavaleiro, J. A. S. *J. Porphyrins Phthalocyanines* **2009**, *13*, 358.
14. Barata, J. F. B.; Neves, M. G. P. M. S.; Tomé, A. C.; Cavaleiro, J. A. S. *J. Porphyrins Phthalocyanines* **2009**, *13*, 415.
15. Maes, W.; Ngo, T. H.; Vanderhaeghen, J.; Dehaen, W. *Org. Lett.* **2007**, *9*, 16.
16. Ngo, T. H.; Nastasi, F.; Puntoriero, F.; Campagna, S.; Dehaen, W.; Maes, W. *J. Org. Chem.* **2010**, *75*, 2127.
17. Bröring, M.; Milsmann, C.; Ruck, S.; Köhler, S. *J. Organomet. Chem.* **2009**, *694*, 1011.
18. Scrivanti, A.; Beghetto, V.; Matteoli, U.; Antonaroli, S.; Marini, A.; Mandoj, F.; Paolesse, R.; Crociani, B. *Tetrahedron Lett.* **2004**, *45*, 5861.
19. Zhan, H. Y.; Liu, H.-Y.; Chen, H.-J.; Jiang, H.-F. *Tetrahedron Lett.* **2009**, *50*, 2196.
20. Rohand, T.; Dolusic, E.; Ngo, T. H.; Maes, W.; Dehaen, W. *ARKIVOC* **2007**, 307.
21. D'Souza, F.; Chitta, R.; Ohkubo, K.; Tasior, M.; Subbaiyan, N. K.; Zandler, M. E.; Rogacki, M. K.; Gryko, D. T.; Fukuzumi, S. *J. Am. Chem. Soc.* **2008**, *130*.
22. Marion, N.; Navarro, O.; Me, J.; Stevens, E. D.; Scott, N. M.; Nolan, S. P. *J. Am. Chem. Soc.* **2006**, *128*, 4101.
23. Leadbeater, N. E.; Resouly, S. M. *Tetrahedron* **1999**, *55*, 1188.
24. Indolese, A. F. *Tetrahedron Lett.* **1997**, *38*, 3513.
25. Lee, C.-C.; Ke, W.-C.; Chan, K.-T.; Lai, C.-L.; Hu, C.-H.; Lee, H. M. *Chem.—Eur. J.* **2007**, *13*, 582.
26. Barder, T. E.; Walker, S. D.; Martinelli, J. R.; Buchwald, S. L. *J. Am. Chem. Soc.* **2005**, *127*, 4685.
27. Kinzel, T.; Zhang, Y.; Buchwald, S. L. *J. Am. Chem. Soc.* **2010**, *132*, 14073.
28. Fors, B. P.; Krattiger, P.; Strieter, E.; Buchwald, S. L. *Org. Lett.* **2008**, *10*, 3505.
29. Sheng, Q.; Hartwig, J. F. *Org. Lett.* **2008**, *10*, 4109.
30. Zim, D.; Buchwald, S. L. *Org. Lett.* **2003**, *5*, 2413.
31. Ghosh, A.; Wondimagegn, T.; Parusel, A. B. J. *J. Am. Chem. Soc.* **2000**, *122*, 5100.
32. Wasbotten, I. H.; Wondimagegn, T.; Ghosh, A. *J. Am. Chem. Soc.* **2002**, *124*, 8104.
33. Brückner, C.; Brinas, R. B.; Bauer, J. A. K. *Inorg. Chem.* **2003**, *42*, 4495.
34. Steene, E.; Dey, A.; Ghosh, A. *J. Am. Chem. Soc.* **2003**, *125*, 16300.
35. Luobeznova, I.; Simkhovich, L.; Goldberg, I.; Gross, Z. *Eur. J. Inorg. Chem.* **2004**, 1724.
36. Guilard, R.; Gros, C. P.; Barbe, J.-M.; Espinosa, E.; Jerome, F.; Tabard, A.; Latour, J.-M.; Shao, J.; Ou, Z.; Kadish, K. M. *Inorg. Chem.* **2004**, *43*, 7441.
37. Pierloot, K.; Zhao, H.; Vancoillie, S. *Inorg. Chem.* **2010**, *49*, 10316.
38. Bröring, M.; Brégier, F.; Tejero, E. C.; Hell, C.; Holthausen, M. C. *Angew. Chem.* **2007**, *119*, 449.
39. Ou, Z.; Shao, J.; Zhao, H.; Ohkubo, K.; Wasbotten, I. H.; Fukuzumi, S.; Ghosh, A.; Kadish, K. M. *J. Porphyrins Phthalocyanines* **2004**, *8*, 1236.
40. Koszarna, B.; Gryko, D. T. *J. Org. Chem.* **2006**, *71*, 3707.
41. Frisch, M. J.; Pople, J. A. *Gaussian 03 Revision C.02 Gaussian*; Gaussian Inc.: Wallingford, CT, 2004.
42. Virko, S.; Petrenko, T.; Yaremko, A.; Wysokinski, R.; Michalska, D. *J. Mol. Struct. (THEOCHEM)* **2002**, *582*, 137.
43. Adamo, C.; Barone, V. *J. Chem. Phys.* **1998**, *108*, 664.
44. Figgen, D.; Rauhut, G.; Doll, M.; Stoll, H. *Chem. Phys.* **2005**, *311*, 227.
45. Peterson, K. A.; Puzzarini, C. *Theor. Chem. Acc.* **2005**, *114*, 283.
46. Casida, M. E.; Jaorski, C.; Casida, K. C.; Salahub, D. R. *J. Chem. Phys.* **1998**, *108*, 4439.
47. *APEX2; Version 2009.9 ed.*; Bruker AXS: USA, 2009; p Software Package.
48. *SAINT; Version 7.68A ed.*; Bruker AXS: Madison, WI, 2009; p Data Integraton Software.
49. Sheldrick, G. M. *Version 2008/1 ed*; Universitat Göttingen: Germany, 1996; p Program for absorption correction with the Bruker SMART system.
50. Sheldrick, G. M. *SHELXS-97 ed*; University of Göttingen: Göttingen (Germany), 1997; p Program for the Solution of Crystal Structures.
51. Sheldrick, G. M. *Acta Crystallogr.* **2008**, *A64*, 112.
52. Spek, A. L. *J. Appl. Crystallogr.* **2003**, *36*, 7.